IMPROVEMENT OF POWER SYSTEM TRANSIENT STABILITY USING WIND FARMS BASED ON A DOUBLY –FED INDUCTION GENERATION (DFIG)

Sabir MESSALTI [1] **Ahmed. GHERBI** [2] **Saad BELKHIAT** [2]
[1] University of M'sila, Faculty of Technology, 28000, M'sila , Algeria, (messalti.sabir@yahoo.fr);
[2] University of Setif, Faculty of Technology, Setif 19000, Algeria

Abstract: This paper describes a new controller of wind power for power system transient stability improvement, which the wind turbine is based on a doubly-fed induction generator (DFIG). A field-oriented control is used to control of the power flow exchanged between the DFIG and the power system. A simplified wind turbine model based on power injection is proposed in this paper. The transient stability is examined with numerical simulations based on relative rotor angles criteria. The Critical Clearing Time is used as an index for evaluated transient stability. The proposed controller is tested in the WSCC3 nine-bus system connected to a wind farms in the case of three-phase short circuit fault on one transmission line for different energy margins injected in power system.

Key words: *Aggregated wind farm model, Critical clearing time CCT, DFIG, Field-oriented control, transient stability.*

1. Introduction

Nowadays, energy crisis and growing environmental consciousness, simultaneously with the industrial growth, have led to an increase in electrical energy consumption. In turn, this has led to a growth in generation and transmission systems to face the increasing demand. Power system has become inherently large and complex. As a consequence, power systems are heavily loaded and also presents new challenges to power system transient stability. Power system stability is the ability to regain an equilibrium state after being subjected to a physical disturbance. Transient stability analysis examines the dynamic behavior of a power system for a period of several seconds following a disturbance [1,2].For many years, a great research interest has focused on improving the transient stability of power system [3-8].

Confronted with a growing energy demand and depletion in the longer term of fossil fuels, different alternatives were considered and many organizations have moved their focus towards renewable energy sources such as wind, solar, hydro, tidal wave, biomass, etc. Wind power is being used as a clean and safe energy resource for electricity generation.

Many types of generators have been used to convert wind power into electricity, especially the Doubly-Fed Induction Generators (DFIG) which is becoming increasingly popular in large wind power conversion systems due to their various advantages. [9,11]. A DFIG in a wind turbine has the ability to generate maximum power with varying rotational speed, to control active and reactive by integration of electronic power converters such as the back-to-back converter, low rotor power rating resulting in low cost converter components, etc. Owing to the decoupled active and reactive control possibilities [12,13], the main area of application for the DFIG is in variable-speed generating systems such as wind power and hydro power [13-14].

Actually wind energy has widely grown; the increasing size of wind farms requires power system stability analysis including dynamic models of the wind power generation. The response of wind turbines during power system disturbances is an important issue, especially since the rated power of wind-turbine installations are steadily increasing. Many papers have treated the use of wind-turbine in improving power system performance [9-11].

This paper presents a basic design of an active power modulation controller which, in the presence of major disturbances in the power system will improve the transient stability. Therefore, in order to balance demand and generation, DFIG have to adjust their power output due to a variable wind power production. Any deficit or excess of power system will be compensated by the DFIG. This paper is organized as follows: The first part studies wind park model and the dynamics of the DFIG model establishing the Field-oriented control strategy with PI current and power controllers [15-17]. The second part shows the modeling of power system with different controllers and regulators. The discussion and analysis are presented in the third part, which the equivalence modeling of a wind park involves combining all turbines with the same mechanical natural frequency into a single equivalent turbine.

2. Modeling of wind generator

2.1. Wind Turbine Model

The mathematical relation for the mechanical power extraction from the wind can be expressed as follows:

$$P_{aer} = \frac{1}{2} C_p(\lambda, \beta) \rho S v_{wind}^3 \quad (1)$$

Where:

P_{aer} is the extracted power from the wind;

ρ : is the air density (kg/m^3);

S : is the turbine swept area (m^2);

v_{wind} : is the wind speed (m/s);

β : Blade pitch angle (deg);

C_p : is the performance coefficient of the turbine, C_p is often given as a function of the tip speed ratio λ;

λ : is the ratio of blade tip speed to wind speed defined by

$$\lambda = \frac{R\Omega}{V_{wind}} \tag{2}$$

Ω: the wind turbine rotational speed (rad /sec);

R: the wind turbine radius.

2.2. Aggregated Model of Wind Park

Wind farms contain many windmills and detailed modeling can be prohibitive due to computational complexity. In order to reduce the complexity of the analysis, a group of identical generators comprising each wind farm can be replaced by an equivalent generator [18-20].

The equivalence modeling of a wind park involves combining all turbines with the same mechanical natural frequency into a single equivalent turbine. Each of these equivalenced turbines is then connected to an equivalent induction generator. The aggregated wind farm model is based on the idea of adding the power of the individual wind turbine. The total mechanical power is:

$$P_m^e = \sum_{i=1}^{ng} P_i = \sum_{i=1}^{ng} \frac{1}{2} Cp_i(\lambda_i, \beta_i)\rho S_i v_{i\,wind}^3 \tag{3}$$

Where *ng* is the number of wind turbine in the wind farm. [18-20].

2.3. Model of Doubly- fed-Induction Generator

The DFIG wind turbines utilize a wound rotor induction generator. The concept is based on two back-to-back voltage source converters connecting the grid and the rotor windings. The stator windings are connected directly to the grid [12-14]. A typical configuration of a DFIG–based wind turbine is shown schematically in Fig. 1. The converter system enables variable speed operation of the wind turbine by decoupling the power system electrical frequency and the rotor mechanical frequency. By a proper adjustment of the voltage applied to the rotor circuits of the doubly-fed induction generator, the speed and consequently the active power can be controlled.

The general model of the DFIG obtained using Park transformation is given by the following equations [15-17]

$$\begin{cases} V_{ds} = R_s.I_{ds} + \dfrac{d}{dt}\phi_{ds} - \omega_s\phi_{qs} \\ V_{qs} = R_s.I_{qs} + \dfrac{d}{dt}\phi_{qs} + \omega_s\phi_{ds} \\ V_{dr} = R_r.I_{dr} + \dfrac{d}{dt}\phi_{dr} - \omega_r\phi_{qr} \\ V_{qr} = R_r.I_{qr} + \dfrac{d}{dt}\phi_{qr} + \omega_r\phi_{dr} \end{cases} \tag{4}$$

$$\begin{cases} \phi_{ds} = L_s.I_{ds} + M.I_{dr} \\ \phi_{qs} = L_s.I_{qs} + M.I_{qr} \\ \phi_{dr} = L_r.I_{dr} + M.I_{ds} \\ \phi_{qr} = L_r.I_{qr} + M.I_{qs} \end{cases} \tag{5}$$

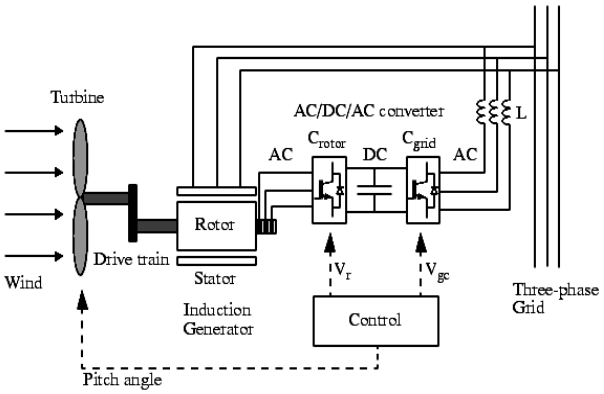

Fig. 1. The Wind Turbine and the DFIG System

The electromagnetic torque and its associated motion equation are expressed respectively by:

$$C_{em} = p\frac{M}{L_s}\left[\varphi_{qs} i_{dr} - \varphi_{ds} i_{qr}\right] \tag{6}$$

$$J\frac{d\Omega}{dt} = C_{em} - C_r - f\Omega \tag{7}$$

2.4. Stator Flux Oriented Control of DFIG

To achieve a stator active and reactive power vector independent control, by orienting the reference (d,q) so that the axis is aligned with the stator flux [15-16], the following solutions can be obtained:

$$\phi_{ds} = \phi_s \quad and \quad \phi_{qs} = 0 \tag{8}$$

$$\begin{cases} \phi_s = L_s.I_{ds} + M.I_{dr} \\ 0 = L_s.I_{qs} + M.I_{qr} \end{cases} \tag{9}$$

$$C_{em} = -p\frac{M}{L_s}\varphi_{ds} I_{qr} \tag{10}$$

$$\begin{cases} V_{ds} = R_s.I_{ds} + \dfrac{d}{dt}\phi_s \\ V_{qs} = R_s.I_{qs} + \omega_s\phi_s \end{cases} \tag{11}$$

By neglecting the stator windings resistance (for high power generators) the stator voltages equations become

$$\begin{cases} V_{ds} = 0 \\ V_{qs} = V_s = \omega_s\phi_s \end{cases} \tag{12}$$

The relation between the stator and rotor currents is set from the equation:

$$\begin{cases} I_{ds} = -\dfrac{M}{L_s} I_{dr} + \dfrac{\phi_s}{L_s} \\ I_{qs} = -\dfrac{M}{L_s} I_{qr} \end{cases} \tag{13}$$

The stator active and reactive power, can be written as:

$$\begin{cases} P_s = V_s I_{qs} = -\dfrac{\omega_s \phi_s M}{L_s} I_{qr} \\ Q_s = V_s I_{ds} = -\dfrac{\omega_s \phi_s M}{L_s} I_{dr} + \dfrac{\omega_s \phi_s^2}{L_s} \end{cases} \quad (14)$$

Substituting currents in equation (5) currents by their values in equations (13) we obtain

$$\begin{cases} \phi_{dr} = \left(L_r - \dfrac{M^2}{L_s} \right) I_{dr} + \dfrac{V_s^2}{L_s \omega_s} \\ \phi_{qr} = \left(L_r - \dfrac{M^2}{L_s} \right) I_{qr} \end{cases} \quad (15)$$

Replacing the flux in the relation (2) we obtain :

$$\begin{aligned} V_{dr} &= R_r . I_{dr} + \left(L_r - \frac{M^2}{L_s} \right) \frac{dI_{dr}}{dt} - g\omega_s \left(L_r - \frac{M^2}{L_s} \right) I_{qr} \\ V_{qr} &= R_r . I_{qr} + \left(L_r - \frac{M^2}{L_s} \right) \frac{dI_{qr}}{dt} + g\omega_s \left(L_r - \frac{M^2}{L_s} \right) I_{dr} + g\omega_s \frac{M \phi_s}{L_s} \end{aligned} \quad (16)$$

Where g is the slip of the induction machine and $\omega_r = g\omega_s$.

In steady state operation the voltage expressions are:

$$\begin{aligned} V_{dr} &= R_r . I_{dr} - g\omega_s \left(L_r - \frac{M^2}{L_s} \right) I_{qr} \\ V_{qr} &= R_r . I_{qr} + g\omega_s \left(L_r - \frac{M^2}{L_s} \right) I_{dr} + g\omega_s \frac{M \phi_s}{L_s} \end{aligned} \quad (17)$$

The independent control of active and reactive powers is shown in Figure.2, the both axes are controlled separately[15-17]. This result is very interesting for wind energy applications to power system transient stability improvement. This technique will be exploited and developed in the following sections.

3. Modeling of Power system

3.1. Modeling of Wind Power Controller

Power production and consumption have to be in balance within a power system. Any variation in power supply or demand can lead to a temporary imbalance in the system and affect operating conditions of power plants as well as affecting consumers. In order to avoid long-term unbalanced conditions the power demand is predicted and power plants adjust their power production

The requirements regarding active power control of wind farms aim to ensure a stable frequency in the system.

The rapid controllability of the DFIG can be used to significantly enhance the power system stability. The equivalence modeling of a wind park involves combining all turbines with the same mechanical natural frequency into a single equivalent turbine [18-19].

The wind power controller that has been used for this purpose is given in figure.3, where k_{wind} and T_{wind} are the gain and time constant of the wind power controller respectively, in which the output power controller (P_{wind}) will be used as specific or reference power to be produced by the DFIG .

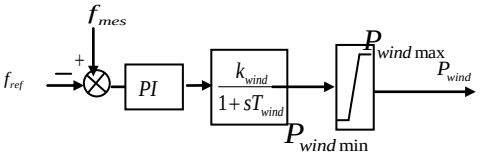

Fig. 3. Model of the wind power controller.

Where : f_{ref} , f_{mes} are the reference and the measured frequency respectively.

The proposed power modulation P_{wind} has been incorporated in the power system in which any deficit or excess of power system is compensated by the DFIG.

The generator system behaviour (linearised model) is governed by the swing Eq.(18) :

$$\frac{d\omega}{dt} = \frac{d^2\delta}{dt^2} = \frac{\pi . f}{H} \left(P_m - (P_e - P_{WIND}) \right) \quad (18)$$

The electric power in power system can be written by:

$$P_e = \left(P_e - P_{wind} \right) \quad (19)$$

It is clear that rapid modulation P_{wind} can significantly improve the transient behavior of the synchronous and damping of oscillations of power system. It is considered that the wind power margins are considered are given by: ($\Delta P_{wind\,min} \le \Delta P \le \Delta P_{wind\,max}$ and $\Delta Q = 0$).

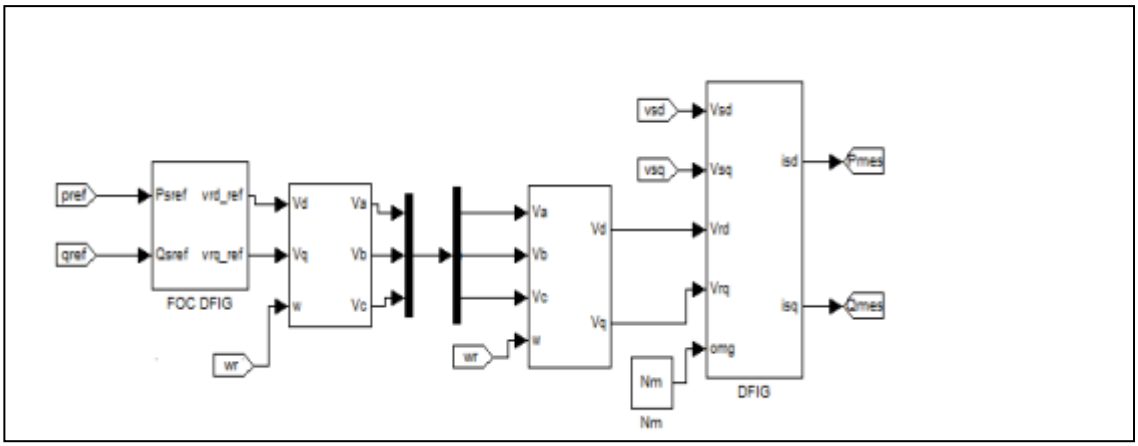

Fig.2. Block diagram of stator-flux-oriented control of a DFIG

3.2. Modeling of Generator

This approach is based on control the frequency of power system by acting on the power delivered by the winds farms. A synchronous machine together with wind turbine can be modeled using the following non-linear dynamic equations [1, 2,4]:

$$\frac{d\delta}{dt} = \omega - 2.\pi.f \tag{20}$$

$$\frac{d\omega}{dt} = \frac{d^2\delta}{dt^2} = \frac{\pi.f}{H}(P_m - (P_e - P_{WIND})) \tag{21}$$

$$\frac{dE_q^{'}}{dt} = \frac{1}{T_{do}^{'}}\left[E_{ex} - E_q^{'} + (X_d - X_d^{'}).I_d\right] \tag{22}$$

$$\frac{dE_d^{'}}{dt} = \frac{1}{T_{qo}^{'}}\left[-E_d^{'} - (X_q - X_q^{'}).I_q\right] \tag{23}$$

The system algebraic equations are given as follows:

$$I_{di} = G_{ij}.E'_{di} + B_{ij}.E'_{qi} + \sum_{\substack{j=1 \\ j\neq i}}^{NG}\left[E'_{dj}.F_{G+B}(\delta_{ij}) + E'_{qj}F_{B-G}(\delta_{ij})\right] \tag{24}$$

$$I_{qi} = G_{ij}.E'_{qi} - B_{ij}.E'_{qi} + \sum_{\substack{j=1 \\ j\neq i}}^{NG}\left[E'_{qj}.F_{G-B}(\delta_{ij}) + E'_{dj}F_{B+G}(\delta_{ij})\right] \tag{25}$$

Where:

$$F_{G+B}(\delta_{ij}) = G_{ij}\cos(\delta_i - \delta_j) + B_{ij}\sin(\delta_i - \delta_j) \tag{26}$$

$$F_{G-B}(\delta_{ij}) = B_{ij}\cos(\delta_i - \delta_j) - G_{ij}\sin(\delta_i - \delta_j) \tag{27}$$

$$V_{di} = E'_{di} - X'_{qi}.I_{qi} \tag{28}$$

$$V_{qi} = E'_{qi} - X'_{di}.I_{di} \tag{29}$$

$$V_i = \sqrt{(V_{di})^2 + (V_{qi})^2} \tag{30}$$

$$Pe_i = E'_{di}I_{di} + E'_{qi}I_{qi} \tag{31}$$

3.3. Modeling of Voltage Regulator

Fig.4 shows the model of Automatic Voltage Regulator used for simulation of the power system:

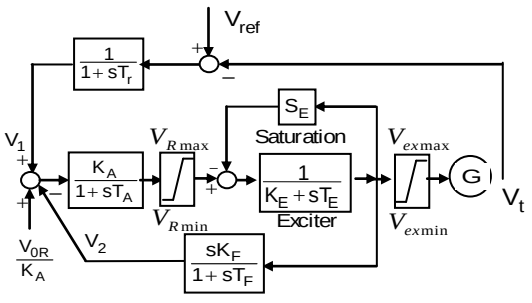

Fig 4. Block diagram of AVR model

It is modeled with three variables: the exciter output voltage V_{ex}, the regulator voltage V_1 and the stabilizer state V_2 related by the following equations:

$$\frac{dV_1}{dt} = \frac{1}{T_r}\left(V_{ref} - V_t - V_1\right) \tag{32}$$

$$\frac{dV_R}{dt} = \frac{1}{T_A}\left[K_A\left(V_1 + \frac{V_{oR}}{K_A} - V_2\right) - V_R\right] \tag{33}$$

$$\frac{dE_{ex}}{dt} = \frac{1}{T_E}\left[V_R - (S_E + K_E)E_{ex}\right] \tag{34}$$

$$\frac{dV_2}{dt} = \frac{1}{T_F}\left(K_F\frac{dE_{ex}}{dt} - V_2\right) \tag{35}$$

3.4. Modeling of Speed Regulator

The speed governor for hydroelectric generators used in this work is illustrated in the block diagram of the figure.5

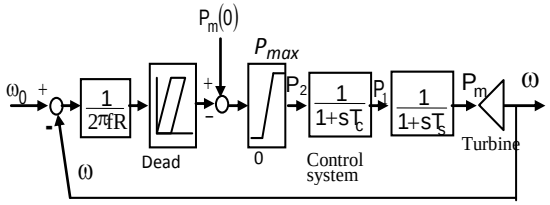

Fig. 5. Block diagram of governor turbine for hydro generator

The state variables of the regulator are related by the following equations:

$$\frac{dP_m}{dt} = \frac{1}{T_S}(P_1 - P_m) \tag{36}$$

$$\frac{dP_1}{dt} = \frac{1}{T_C}(P_2 - P_1) \tag{37}$$

$$P_2 = P_m(0) - \frac{1}{R}\left[\frac{\omega_b - \omega}{2\pi f} \pm DBt\right] \tag{38}$$

4. Algorithm of Transient Stability Analysis

The steps of the algorithm used for transient stability analysis of power system are the following[4]:

•Modeling of the network (power system, regulators, loads, , wind turbine, FACTS,..etc);

•Initialization of AC data;

•The computation of load flow using gauss-seidel.

•Compute the prefault system admittance matrix ($Y_{prefault}$) and reduced admittance matrix (N_G x N_G) where N_G is the number of generator;

•The computation of initial conditions for differential equations describing the dynamic of power system;

• At t = 0, the three phase fault is occurred at bus and persists until the fault is cleared at t=Td; (the system is considered stable before the fault);

•Compute the faulted system admittance matrix (Y_{fault}) and reduced admittance;

•Solve all differential equations taking into account the admittance matrix for each step using the Runge-kutta method with the inclusion of the effect of wind turbine connected to the power system (before, during and after fault) ;

• At t=Td, isolate the line on which the fault occurred;

• Compute the post fault system admittance matrix ($Y_{postfault}$) and reduced admittance matrix;

• Solve all differential equations taking into account the admittance matrix for each period using the Runge kutta's

method with the inclusion of the effect of wind turbine;
• Plot the relative rotor angles and all parameters;
• Assessment transient stability using relative rotor angles criterion and assessment of CCT.

5. Results Analysis

The feasibility and efficiency of the proposed controller have been tested on a modified 9-bus 3-machine test system connected to a wind farms as shown in Fig.6. A three-phase fault is applied on one transmission line and cleared by disconnecting the affected line. Transient stability is tested for different energy margin injected in power system. Relative rotor angles criterion is used for transient stability assessment based on Runge- Kutta method. The optimal value of the CCT is determined by trial and error. For this, several values of the length of the fault duration (Td) are preselected and the Td is increased with very small steps until the system becomes unstable.

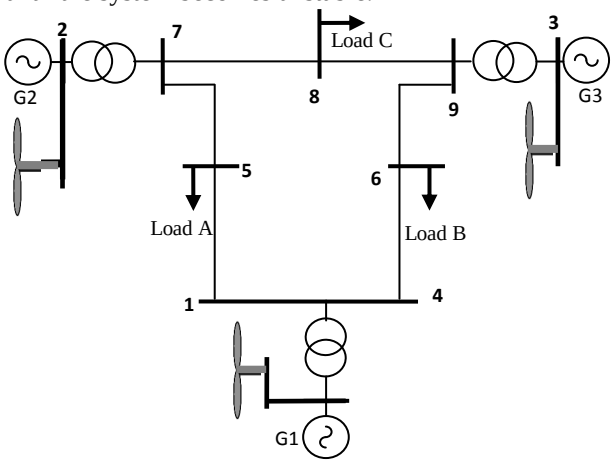

Fig. 6. A Three machines power system with wind generator

4.1. Transient Stability Assessment Without Wind Turbine

Simulation results for three-phase short circuit on the line 7-8 near the bus 8 without wind power injection are presented in following figures:

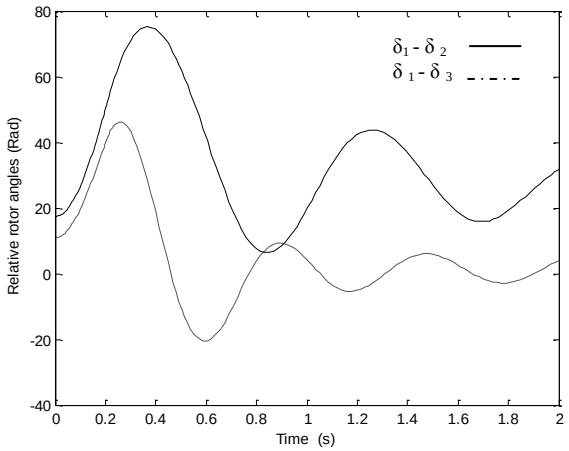

Fig. 7. Relative rotor angles without wind power (Td=0.210s)

Figure.7 and Figure.8 show respectively the relative rotor angles and frequency for Td=0.210s. The relative rotor angles are oscillatory damped, frequencies of the three machines converge to the same frequency, so the system is stable.

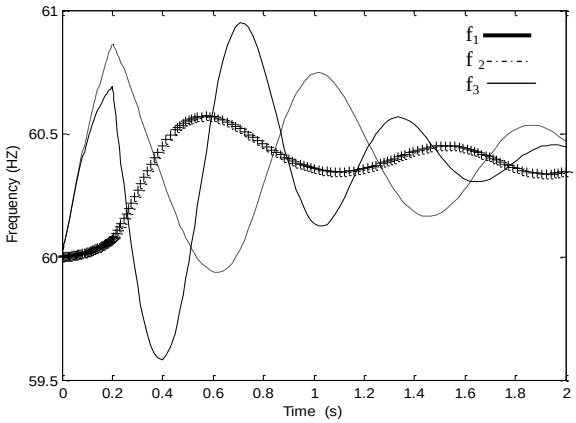

Fig. 8. Frequency (Td=0.21s)

In Figure 9, it's clear that the relative rotor angles are not oscillatory damped, Figure.10 shows the three frequencies become asynchronous and stability is lost.

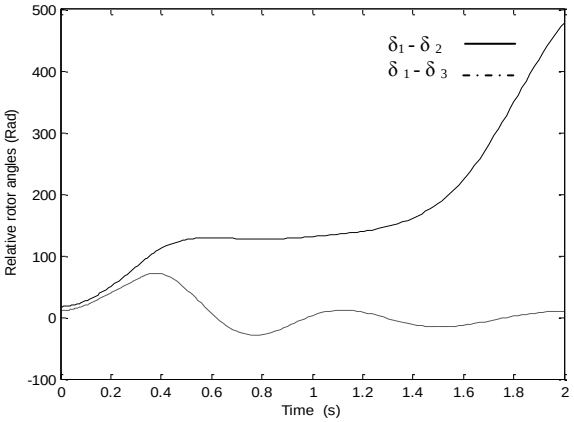

Fig. 9. Relative rotor angles without wind power (Td=0.331s)

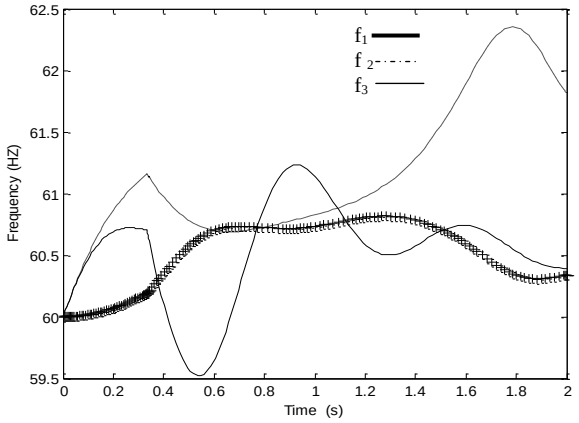

Fig. 10. Frequency without wind power (Td=0.331s)

4.2. Effect of Wind turbine on power system

Transient stability

In order to demonstrate the interaction between the wind farms and the transient stability improvement, simulation results for three-phase short circuit on the line 7-8 near the bus 8 with different active wind margins injected in power system are presented in following figures:

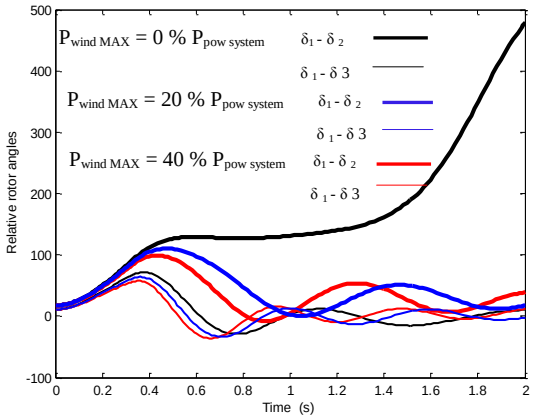

Fig. 11. Relative rotor angles with different wind power margin injected (Td=0.333s)

Figure.11 shows the relative rotor angles for Td=0.331s in which the system was unstable. It can be observed that the system becomes again stable with wind power injection.

Results obtained with Runge-Kutta method are indicated in Table 1, in which the penetration level is the ratio between the total active power of all wind farms installed and the total power of the power system.

In comparison, the system performance with active wind power modulation is better, the results indicate that the wind power control can significantly improve the oscillation and increase the CCT.

Table 1. CCT for various wind power injected (P_{wind}) in power system

Wind Power (MW)	$P_{wind\ max}$	CCT(s)
0	0	0.331
16	5%	0.358
32	10%	0.376
64	20%	0.401
96	30%	0.405
128	40%	0.432

5. Conclusion

In this paper, a new control strategy of wind power has been successfully applied to improve the power system transient stability. The aggregated wind farm model is used for wind farms modeling. The input power to the DFIG is computed at each integration step. Results indicate that the wind power control can significantly improve the oscillation and increase the CCT, the efficiency of the wind farms is more important when the percentage of the installed wind power over the total production is higher.

References

[1] P. Kundur, *Power System Stability and Control*: McGraw-Hill, 1994.

[2] P. M. Anderson and A. A. Fouad, *Power System Control and Stability*, New York: IEEE Press, sec. Revised Printing, 1994.

[3] S. Messalti, I. Griche, A. Gherbi, and S. Belkhiat "*Thyristor Controlled Voltage Regulator and Thyristor Controlled Phase Angle Regulator for Transient Stability Improvement of AC-HVDC Power System*",Adv. Sci. Lett. 19, 1421-1425 (2013).

[4] S. Messalti, S. Belkhiat, S. Saadate, D. Flieller, "*Improvement of Power System Transient Stability Using TCSC and TCBR, A Comparative study* ", International Review of Electrical Engineering, vol. 5, n. 6, 2010, pp 2727-2736

[5] D.J. Sobajic, Y.H. Pao,"*Artificial neural-net based dynamic security assessment for electric power system*" Power Systems, IEEE Transactions on , vol.4, no.1, pp. 220-228, Feb 1989

[6] A. Gherbi, B. Francois, M. Belkacemi, *Methods for power system transient stability analysis, State of the art*, Electrical and Computer Engineering, Canadian Journal 2006, 311, 3-13.

[7] L. Seung-Cheol, M. Seung, "*Hybrid linearization of a power system with FACTS devices for a small signal stability study: Concept and application*", Electric Power Systems Research, vol. 64, n. 1, 2003, pp. 27-34.

[8] G. A. Maria, C. Tang, J. Kin, *Hybrid transient stability analysis*, Transactions on Power Systems, vol. 5, n. 2, 1990, pp. 34-39.

[9] V. Akhmatov, "*Variable-speed wind turbines with doubly-fed induction generators. Part IV: Uninterrupted operation features at grid faults with converter control coordination*," Wind Energy, 2003, vol. 27, pp. 519–529

[10] S. Muller, M. Deicke, , R. W. De Doncker, "*Doubly fed induction generator systems for wind turbines*", *IEEE Ind. Appl. Mag, vol. 8, n.3, Jun. 2002* , pp. 26–33

[11] Y. Lei, A. Mullane, G. Lightbody, R. Yacamini, "*Modeling of the Wind Turbine with a Doubly Fed Induction Generator for Grid Integration Studies"*,

IEEE Trans. Energy Conversion, vol. 21, n. 1, March 2006, pp. 257 – 264.

[12] W . Leonard, "*Field oriented control of a variable speed alternator connected to the constant frequency line*", Proceedings of the IEEE Conference on control of power system, 1979, pp. 149-153

[13] M. Yamamoto and O. Motoyoshi, "*Active and reactive power control for doubly-fed wound rotor induction generator*", IEEE Trans. Power Electron., vol. 6, n. 4, Oct. 1991, pp. 624–629.

[14] R. Pena, J.C. Clare, G.M. Ashek , "*Doubly-fed induction generator using back-to-back PWM converters and its application to variable-speed wind-energy generation*", *Electric Power Applications , IEE Proceedings, vol. 143, n. 3,* 1996, pp. 231-241.

[15] F. Poitiers, M. Machmoum, R. L. Doeuff, M. E. Zaim, "*Control of a doubly-fed induction generator for wind energy conversion systems*", International Journal of Renewable Energy Engineering, December 2001, pp. 373–378.

[16] A. Naamane, N.K. Msirdi, "*Doubly-fed induction generator control for an urban wind turbine", International Renewable Energy Congress* November 2010 , Sousse, Tunisia

[17] Z. Boudjema, A. Meroufel , E. Bounadja," *Robust Control Improvement of a Doubly Fed Induction Generator for Wind Energy Conversion",* 4th *International Conference Electrical Engineering*, ~ ICEE' 2012~, Algiers.

[18] J. Khan, *Modeling a wind generator farm for transient stability using equivalencing, M.S*. thesis, Montana Tech, Univ. of Montana, Butte, MT, 2003.

[19] F. Nozari, M. D. Kankam, and W. Price, "*Aggregation of induction motors for transient stability load modeling*," *IEEE* Power Systems, IEEE Transactions on, vol. 2 , n. 4 , Nov. 1987, pp. 1096–1102.

[20] D.J. Trudnowski, A. Gentile; J.M. Khan; E.M. Petritz, "*Fixed-Speed Wind-Generator and Wind-Park Modeling for Transient Stability Studies*",Power Systems, IEEE Transactions on vol. 19 , n. 4 , November 2004, pp. 1911 - 1917

Appendix

P_s , Q_s	Active and reactive stator power,
f	Coefficient of viscous frictions,
C_r	Load torque,
C_{em}	Electromagnetic torque.
I_{ds} , I_{qs}	Two-phase stator currents,
I_{dr} , I_{qr}	Two-phase rotor currents,
V_{ds} , V_{qs}	Two-phase stator voltages,
V_{dr} ,V_{qr}	Two-phase rotor voltages,
φ_{ds} , φ_{qs} ,	Two-phase stator fluxes,
φ_{dr} , φ_{qr}	Two-phase rotor fluxes,
Rs , Rr	Per phase stator and rotor resistances,
L_s , L_r	Per phase stator and rotor inductances,
M	Mutual inductance,
p	Number of pole pairs,
J	Inertia,
D_i	Damping constant of i^{th} generator,
E'_{di}	d-axis transient emfs of i^{th} generator;
E'_{qi}	q-axis transient emfs of i^{th} generator;
H_i	Inertia constant of i^{th} generator,
I_d	d-axis generator currents of i^{th} generator,
I_q	q-axis generator currents of i^{th} generator,
p_{mi}	Mechanical input power of i^{th} generator,
P_{ei}	Electrical power of i^{th} generator,
T'_{d0i}, T'_{q0i}	d-axis and q-axis transient time constants of i^{th} generator,
V_{ex}	Field voltage controlled by a voltage regulator of i^{th} generator,
x'_{di}, x'_{qi}	d-axis and q-axis generators' transient reactance of i^{th} generator,
δ_i	Rotor angle of i^{th} generator,
ω_b	Rotating angular velocity,
ω_i	Rotor angular velocity of i^{th} generator,
R	Speed regulation,
T_c , T_s	Time constants regulator,
P_m	Mechanical power,
$P_m(0)$	Initial mechanical power;
P_1 , P_2	Intermediate state variables,
DB_t	Dead band,
K_R	Regulator gain,
K_A	Amplifier gain,
K_E	Exciter gain,
K_F	Stabilizer gain,
T_R ,	Time constant of regulator ,
T_A	Time constant of amplifier,
T_E	Time constant of exciter,
T_F :	Time constant of stabilizer,
V_1	Regulator output voltage,
V_{or} :	Initial amplifier output voltage,
V_R	Amplifier output voltage,
V_t	Stator voltage,
V_2	Stabilizer output voltage,
V_{di} , V_{di}	d-axis and q-axis of i^{th} generator,